Chapter

Reliability and Comparison of Some GEANT4-DNA Processes and Models for Proton Transportation: An Ultra-Thin Layer Study

Gabriela Hoff, Raquel S. Thomaz, Leandro I. Gutierres, Sven Muller, Viviana Fanti, Elaine E. Streck and Ricardo M. Papaleo

Abstract

This chapter presents a specific reliability study of some GEANT4-DNA (version 10.02.p01) processes and models for proton transportation considering ultra-thin layers (UTL). The Monte Carlo radiation transport validation is fundamental to guarantee the simulation results accuracy. However, sometimes this is impossible due to the lack of experimental data and, it is then that the reliability evaluation takes an important role. Geant4-DNA runs in an energy range that makes impossible, nowadays, to perform a proper microscopic validation (cross-sections and dynamic diffusion parameters) and allows very limited macroscopic reliability. The chemical damage cross-sections reliability (experiment versus simulation) is a way to verify the consistency of the simulation results which is presented for 2 MeV incident protons beam on PMMA and PVC UTL. A comparison among different Geant4-DNA physics lists for incident protons beams from 2 to 20 MeV, interacting with homogeneous water UTL (2 to 200 nm) was performed. This comparison was evaluated for standard and five other optional physics lists considering radial and depth profiles of deposited energy as well as number of interactions and stopping power of the incident particle.

Keywords: Geant4-DNA, Monte Carlo methods, Proton transportation, Ultra-thin layer, Software reliability

1. Introduction

The Monte Carlo toolkit Geant4 [1–3] was developed as a general-purpose transportation toolkit. This toolkit has a framework that extends the transport process to model the early biological damage induced by ionizing radiation at cellular and sub-cellular scale [4–6], the so called Geant4-DNA [4–6], that makes possible to simulate the physical–chemical and chemical processes for water

radiolysis, the molecular geometries, and the damage quantification. This framework can simulate energies from 10 eV to 100 MeV for protons, enabling the simulation of particles' interaction using discrete models at nanoscale. It is also known and well informed on Geant4 manual "Guide For Physics Lists" that simulation of transport for energies below 1 keV reduces significantly the accuracy of the transport models [7]. However, to get a simulation in the necessary scale for Geant4-DNA it is inevitable to consider energies below 1 keV. It allows to simulate, depending on the interacting particle and energy range, the following processes (applying different possible models): elastic scattering, ionization, excitation, electron capture, nuclear scattering, charge increase and decrease, attachment and vibrational excitation [8].

The validation (macroscopic and microscopic) of the results by comparing the Geant4-DNA cross sections or simulated quantities to experimental data is still extremely limited, considering the energy range used by Geant4-DNA, which makes important to be careful on generalizing the simulation results.

In this chapter simulations results of 2 MeV kinetic energy protons impinging on homogeneous water ultra-thin layers (UTLs), using different physics lists (including Geant4-DNA running on version 10.02.p01) are presented. The reliability evaluation was performed considering chemical damage cross section (CDCS) and stopping power (SP). The comparison among different Geant4 recommended physics lists was based on radial and depth deposited energy profiles, number of interactions and SP.

2. The experimental and simulation definitions

In this section the experimental setup, the developed application for the simulation and the results are presented. The strategy used to evaluate the reliability of the simulation for each physics list was performed comparing simulated-calculated to experimental CDCS, and simulated SP to NIST database. The physics lists evaluation was based on the comparison of the results of interaction files generated, that registered several information on each simulation step.

2.1 The experimental setup for chemical damage cross section estimation

The experimental setup used on reliability evaluation was defined to collect the CDCSs using polymer ultra-thin films. High-grade poly(methyl methacrylate) (PMMA) with density 1.190 g/cm^3 and poly(vinyl chloride)(PVC) with density 1.406 g/cm^3 powder were dissolved and spun onto polished silicon (Si) wafers. Homogeneous ultra-thin films, with thicknesses from 4 nm to 200 nm, and very low roughness (∼0.3 nm RMS) were obtained. The films were bombarded by 2 MeV H^+ in vacuum at a HVEE 3 MV Tandetron (Porto Alegre, Brazil) with a set of fluences ranging from 10^{14} ions/cm^2 to 2.8x10^{15} ions/cm^2. X-ray photo-electron spectroscopy (XPS) was performed on the irradiated samples at Universit de Namur, Belgium, to evaluate bond-breaking cross sections of C=O and C-Cl bonds as a function of the thickness of the polymer. The radiolytic efficiency is usually estimated measuring CDCSs for different transformation processes induced by radiation such as bond-breaking [9–11]. These CDCSs for bond-breaking represent the energy loss by length (dE/dx) [12, 13] and are based on the number of specific bond-breaking at the end of an irradiation process. Additional information about the experimental data collection can be found at [14].

2.2 The Monte Carlo simulation

This Geant4-DNA application (version 10.02.p01) was developed considering a protons beam impinging normally on the entrance surface of an ultra-thin layer (UTL) of water in a semi-infinite configuration of 500 nm per 500 nm with thicknesses from 2 nm to 200 nm and a water 500 nm substract. The simulated protons beams were monodirectional and monochromatic with initial kinetic energies of 2 MeV, 5 MeV, 10 MeV and 20 MeV.The CDCS evaluation was performed only for the 2 MeV incident protons beam, while the SP one was performed for 2 MeV, 5 MeV, 10 MeV and 20 MeV protons beams. For each UTL and beam energy 10^5 histories were simulated, taking into account a cut-off of 1 nm for secondary particle generation. According to Geant4-DNA official webpage the Geant4-DNA processes are all discrete; as such, they simulate explicitly all interactions and do not use any production cut, so this 1 nm cut will have no effect on the Geant4-DNA Physics results [8]. The class G4EmDNAPhysics (henceforth named DNA) and the other five available physics lists (named DNAopt1 to DNAopt5) were evoked for each setup configuration for both reliability and comparison studies. So, to enlighten the physics lists evoked to transport protons and electrons, the processes and models used on Geant4-DNA classes are presented on **Figures 1** and **2**.

To simulate the processes and models above cited, additional electromagnetic physics builders are needed and, to support the simulation, the Livermore physics list was implemented by default [15].

Since Geant4-DNA only simulates standard liquid water as interaction material, the only way to explore situations close to the experimental setup was by altering the water density. So, different CDCSs were simulated-calculated using water with different densities. In addition to standard liquid water, composed by 2 hydrogen and 1 oxygen with density of 1 g/cm^3, a "dense water" of the same composition but with a 1.190 g/cm^3 density was considered.

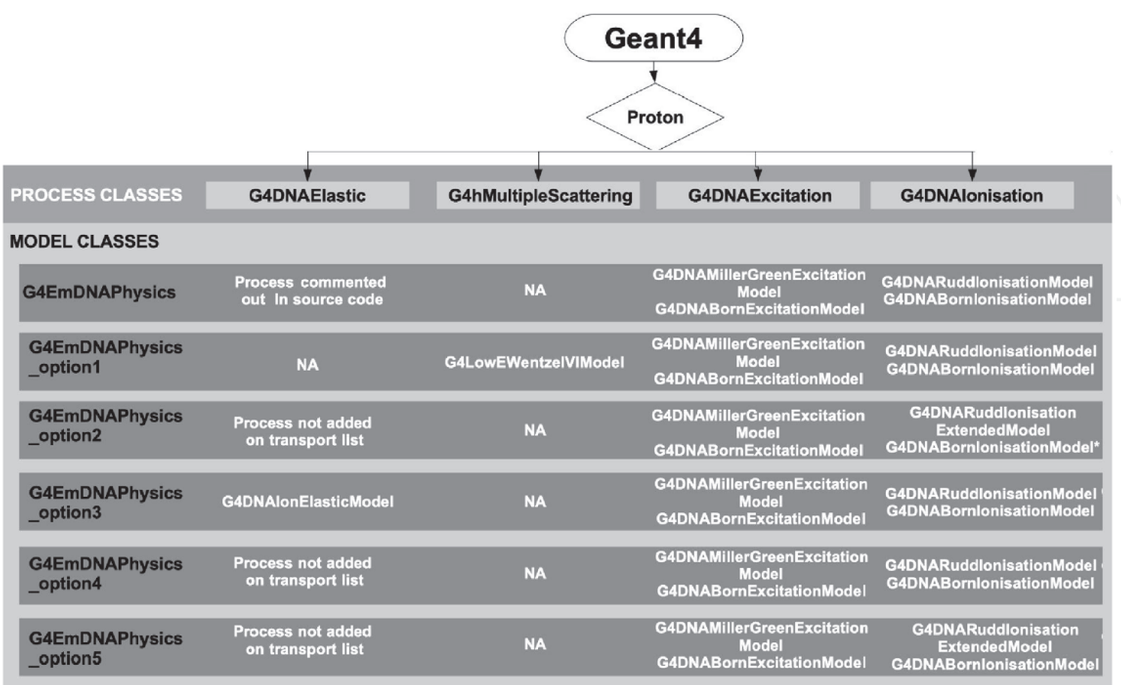

Figure 1.
*Scheme of the processes and models for protons transport and different physics lists. The symbol * indicates that the flag "SelectFasterComputation" was activated. The G4DNAChargeDecrease class always evoke the G4DNADingfelderChargeDecreaseModel class, so it was nod added to the scheme.*

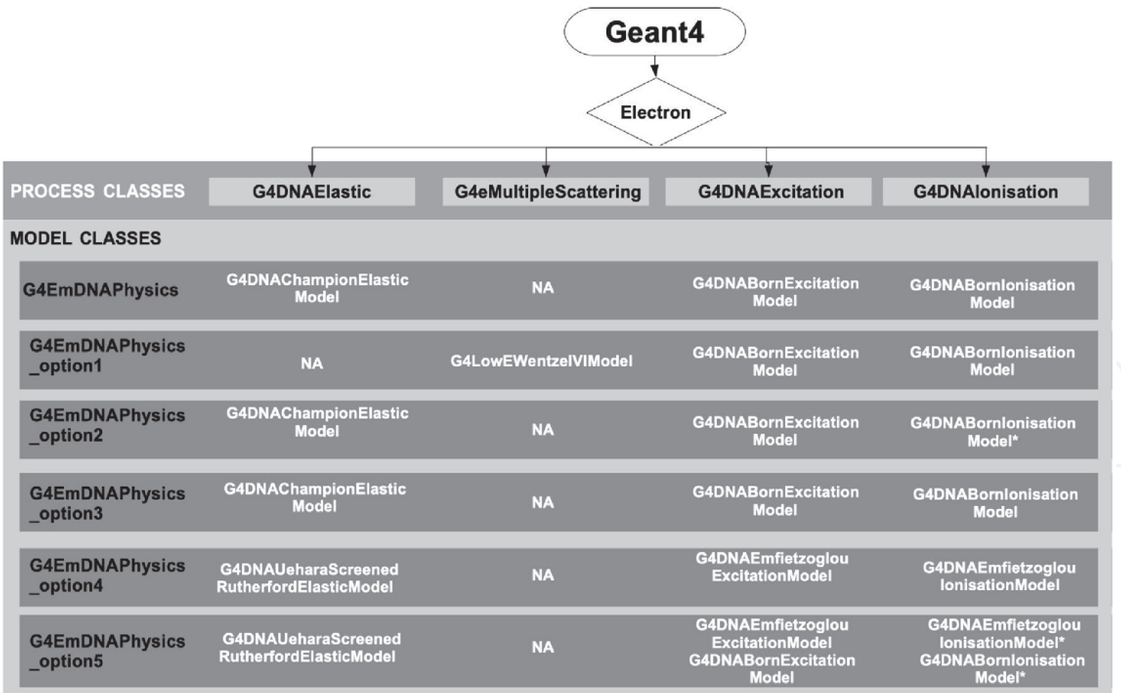

PROCESS CLASSES	G4DNAElastic	G4eMultipleScattering	G4DNAExcitation	G4DNAIonisation
MODEL CLASSES				
G4EmDNAPhysics	G4DNAChampionElastic Model	NA	G4DNABornExcitation Model	G4DNABornIonisation Model
G4EmDNAPhysics _option1	NA	G4LowEWentzelVIModel	G4DNABornExcitation Model	G4DNABornIonisation Model
G4EmDNAPhysics _option2	G4DNAChampionElastic Model	NA	G4DNABornExcitation Model	G4DNABornIonisation Model*
G4EmDNAPhysics _option3	G4DNAChampionElastic Model	NA	G4DNABornExcitation Model	G4DNABornIonisation Model
G4EmDNAPhysics _option4	G4DNAUeharaScreened RutherfordElasticModel	NA	G4DNAEmfietzoglou ExcitationModel	G4DNAEmfietzoglou IonisationModel
G4EmDNAPhysics _option5	G4DNAUeharaScreened RutherfordElasticModel	NA	G4DNAEmfietzoglou ExcitationModel G4DNABornExcitation Model	G4DNAEmfietzoglou IonisationModel* G4DNABornIonisation Model*

Figure 2.
*Scheme of the processes and models for electron transport and different physics lists. The symbol * indicates that the flag "SelectFasterComputation" was activated. The G4DNAAttachment and G4DNAVibExcitation classes always evoke respectively the G4DNAMeltonAttachmentModel and the G4DNASancheExitationModel classes, so it was nod added to the scheme.*

The total number of histories, the total deposited energy and its statistical fluctuations were recorded at the end of each run. Also, during the simulation, for each interaction, the following information were recorded: pre and post-step position (x, y and z, in nm); deposited energy due to the interaction (in MeV); event, parent particle, track and step identification; process name and particle type. Later, these information were organized/accumulated on bins representing radial deposited energy profiles (henceforth called radial profile) and SP obtained with different physics lists.

To estimate the CDCS, radial profiles based on the position information recorded for 2 MeV incident kinetic energy protons beam and thicknesses from 2 nm to 200 nm were generated. The SP for protons was calculated considering the total energy deposited in each UTL divided by its thickness.

2.3 The reliability evaluation

On this subsection the methodological strategy used and the results for the reliability evaluation are presented.

The CDCS was calculated based on the standard thermally activated model (STAM) [16] taking into account the radial deposited energy profile simulated to generate the probability energy deposition function which was adjusted to estimate the activation energy density value for a specific bond-break in N positions [14]. The simulated-calculated CDCS was compared to experimental ones for 2 MeV H^+ on PMMA and PVC ultra-thin films.

The SP profile as function of the UTL thickness was evaluated by the fitting curve considering all thicknesses for each incident kinetic energy protons beam and each physics list. The fitting TamLog (y = a + b*ln(sing*(x-c))) for all curves presented R-squared coefficient larger than 0.99. The radial profile, mainly formed by secondary electrons, was used to define the simulated electron range which was compared to the CSDA ESTAR electrons range [17]. The simulated SP is a microscopic quantity

since the largest water UTL thickness is smaller than the expected electron range which is a limitation in this comparison, but unfortunately it was not possible to find an experimental SP database valid for ultra-thin layers. This comparison was performed using the extrapolation of the fitting TamLog curve considering the macroscopic CSDA ESTAR electrons range as a limit. The NIST CSDA ESTAR electrons range was defined based on the calculated maximum kinetic energy (K_{max}) that can be transferred in a head-on collision with an atomic electron. The Eq. (1) [18] depends on the relativistic velocity parameter of the incident proton ($\beta = \frac{v_{incidentparticle}}{c}$) and the rest-mass energy of the scattered electron (m_0c^2).

$$K_{max} \simeq 2m_0c^2\left(\frac{\beta^2}{1-\beta^2}\right) \quad (1)$$

This equation assumes that the electrons are unbound and is applicable for an incident heavy particle with kinetic energy smaller than its rest-mass energy M_0c^2, which is the condition applied to the study case presented in this chapter. The K_{max} was used as input parameter to estimate the CSDA range from ESTAR database [17], using a log–log interpolation to calculate the data not presented on the database grid. The CSDA ranges estimated from ESTAR were considered maximum limits taking into account the theoretical limitation of the interaction with unbounded electrons. This overestimates electrons range value and limits the comparison between the microscopic simulated range, based on SP, and the macroscopic ESTAR CSDA range. Both conditions underestimate the simulated electrons range and if the simulated value is larger than the ESTAR value, the former is unreliable.

2.3.1 Reliability results based on chemical damage cross section

On this subsection the reliability for the CDCS and the SP considering different Geant4-DNA physics lists are presented and analysed. **Figures 3** and **4** present the

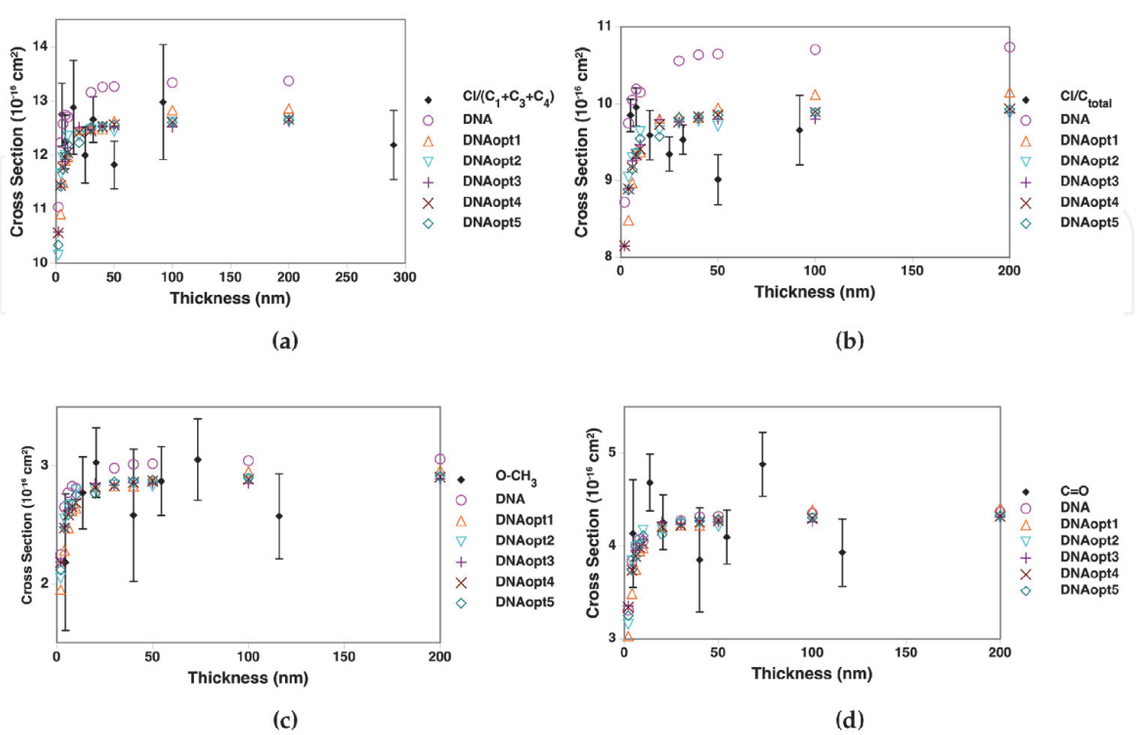

Figure 3.
Chemical damage cross section as function of the UTL thickness considering 2 MeV, bin size of 1 nm and standard water density for bonds $Cl/(C_1+C_3+C_4)$ (a), Cl/C_{total} (b), $O\text{-}CH_3$ (c) and O=C (d) and all physics lists.

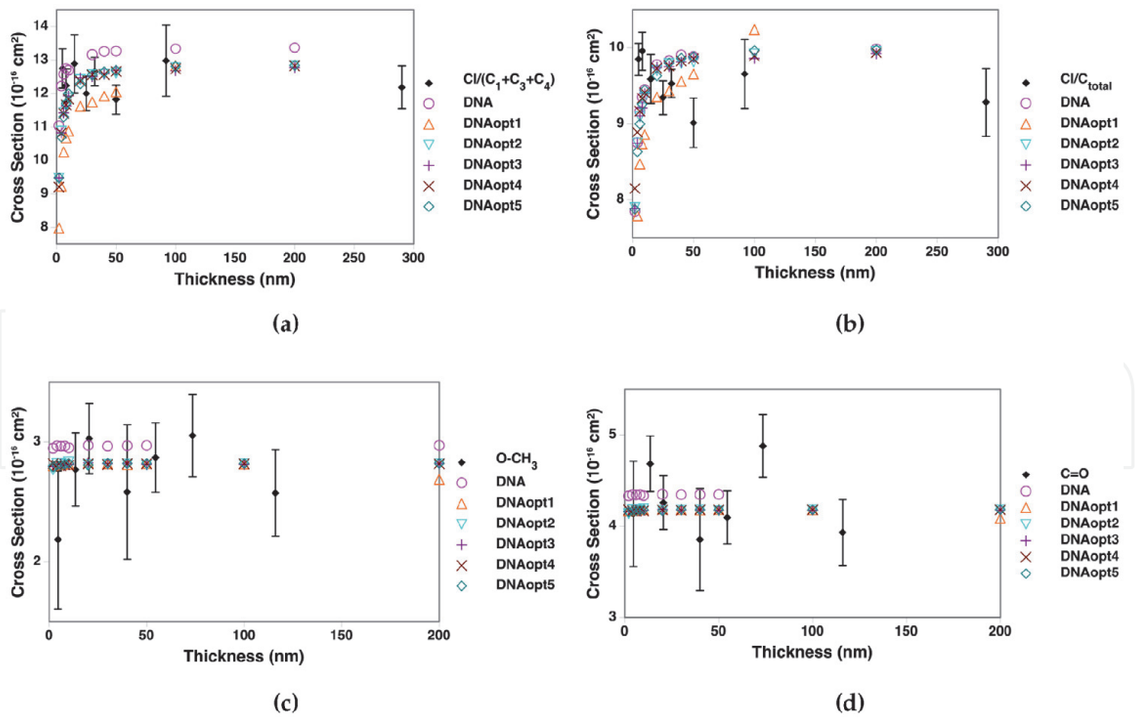

Figure 4.
Chemical damage cross section as function of the UTL thickness considering 2 MeV, bin size of 0.2 nm and standard water density for bonds $Cl/(C_1+C_3+C_4)$ (a), Cl/C_{total} (b), $O\text{-}CH_3$ (c) and O=C (d) and all physics lists.

experimental and simulated data for CDCS and **Table 1** presents the activation energy density considering different bond-breaking for 2 MeV kinetic energy protons beam. Adapting the activation energy published by [10] to the conditions used

	0.2 nm		1.0 nm	
Condition	**$Cl/(C_1+C_3+C_4)$**	**Cl/C_{total}**	**$Cl/(C_1+C_3+C_4)$**	**Cl/C_{total}**
water_DNA	2.21	2.60	4.71	5.12
dense_water_DNA	3.14	3.70	6.07	6.65
water_DNAopt1	2.33	2.73	4.69	5.13
water_DNAopt2	2.21	2.62	4.82	5.29
water_DNAopt3	2.21	2.61	4.82	5.29
water_DNAopt4	2.53	2.98	5.10	5.60
water_DNAopt5	2.53	2.98	5.11	5.60
Condition	$O\text{-}CH_3$	C=O	$O\text{-}CH_3$	C=O
water_DNA	26.45	13.01	7.53	6.84
dense_water_DNA	34.26	17.45	9.62	8.66
water_DNAopt1	27.37	13.91	7.43	6.69
water_DNAopt2	28.32	14.41	7.63	6.87
water_DNAopt3	28.34	14.42	7.64	6.87
water_DNAopt4	29.13	14.82	8.09	7.28
water_DNAopt5	29.08	14.80	8.08	7.28

Table 1.
Calculated values of activation energy density (ε_0), in eV/nm³, for each bond-break situation and condition simulated.

in this study case, the activation energy to get a reliable result must be in the range from 1 eV/nm^3 to 10 eV/nm^3. To analyse the influence of the radial profile step size on CDCS, these profiles were organized in steps of 0.2 nm and 1.0 nm for all studied cases. These two different bins were defined to explore the influence of the extremely strong slope in the first 3 nm of the radial profile curve, where the deposited energy is reduced approximately between 8% and 13% of the total deposited energy, depending on the kinetic energy protons beam.

The CDCSs for water, 1 nm bin size and all transport models for each ultra-thin layer are presented on **Figure 3**. On this figure it is visible that most of the transport models showed the same profile for CDCS as function of the UTL thickness, with the exception of Cl bond-breaks (**Figure 3a** and **b**) and DNAopt1 that showed similar tendency but different amplitude. A similar behaviour for different physics lists can be seen on **Figure 4**, including the DNAopt1 discrepancy observed on CDCSs for 0.2 nm bin size and all physics lists. However, for a complete reliability evaluation it is important to take into account the activation energy used to get the best fitting curve on the estimation of the simulated CDCS (**Table 1**).

Still considering the 0.2 nm bin (**Figure 4**), there is a visible difference on the activation energy values when compared to 1 nm bin. As one can see, the results of activation energy are out of the reliability range presented by [10] for the bonds O-CH_3 and O=C and 0.2 nm bin (**Table 1**). However, it is important to notice that these results are dependent on the accentuated slope of the radial profile discussed on subsection 2.2 which leads to the condition that small changes on the bin size may result in a large change on the activation energy. It is necessary to take this observation into account on further evaluations and to use the most conservative methodology to guarantee the reliability of the results. In this chapter, the total deposited energy calculated for 1 nm bin are reliable because this results presented smaller statistical fluctuations than the ones calculated for 0.2 nm bin, keeping the consistency for the activation energy calculated value.

The dense water when compared to standard water presented, in general, lower CDCSs values, as was expected, due to the increase on this material density.

The activation energies defined to get the best fitting presented on **Table 1** showed values larger than 10 eV/nm^3, out of the reliability range, for bin size 0.2 nm and bond-breaks O-CH3 and C = 0. However, for bin size 1 nm (**Figure 3**) all activation energies evaluated for all bond-breaks are in the reliability range. This significant difference in the activation energy shows the dependency of the CDCS on the bin size defined to generate the radial profile. This happens due to the accentuated slope on the simulated radial profile (**Figure 7b**) where most of the deposited energy is absorbed in the first 5 nm. Because of that, the interpolation method used to integrate the radial deposited energy and its agreement with the simulated data are fundamental.

Another important consideration about CDCS is the shape of the curves for different bin sizes and same bond. In this cases, specially the O=C and O-CH_3 (**Figure 3c, d, 4c** and **d**), the changes on the curve shapes are visible, where 0.2 nm bin presented a flat shape curve which is less reliable based on the experimental data.

To evaluated the effect of material density on CDCS and to observe a condition closer to the experiment setup (PMMA material), the data obtained with dense and standard water were compared to the experimental data. It is visible that the standard water data presented only one case (**Figure 5c**) out of the region defined by the error bars of the experimental CDCS, Cl/C_{total}. Considering the activation energy (**Table 1**) one may see that the values presented by dense water DNA were always larger than the ones presented by standard water DNA. Despite the differences, both descriptions of water presented activation energies in the reliability range, however, taking into account the standard water that presented one case

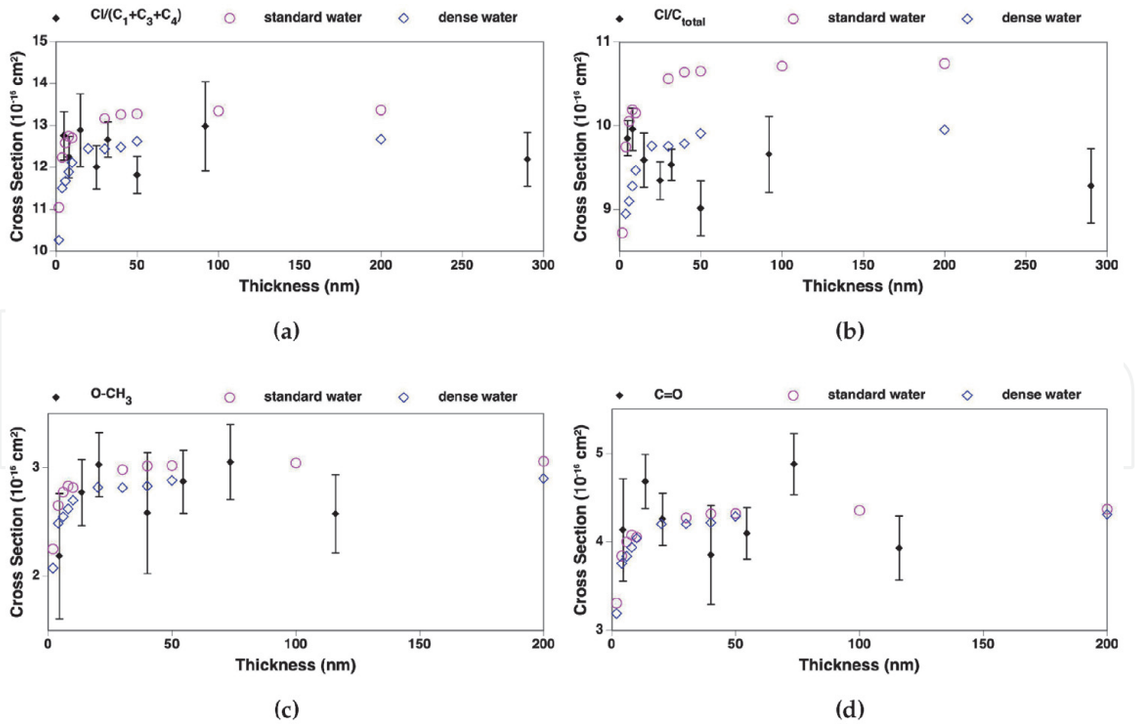

Figure 5.
Chemical damage cross section as function of the UTL thickness considering 2 MeV, different water description, bin size of 1 nm and bonds $Cl/(C_1+C_3+C_4)$ (a), Cl/C_{total} (b), $O\text{-}CH_3$ (c) and O=C (d) simulated with DNA physics list.

(**Figure 5c**) out of the error bars of the experimental CDCS, one may assume that the dense water may be a better option to describe PMMA on simulations.

2.3.2 Reliability based on stopping power

Figure 6 presents the SP values as function of the UTLs for all evaluated energies. All values of SP based on simulated deposited energy were sub-estimated, as expected, since the thickness of the UTLs were inferior to the electron range. According to ESTAR - of National Standards and Technology [17] the observed tendencies for SP at 2 MeV incident protons will achieve the (macroscopic) value for thicknesses around a few hundred nm. For energies of 5 MeV, 10 MeV and 20 MeV differences of 8%, 10% and 18%, respectively, were observed. One can see that the percentage difference increased with the increase on proton incoming energy. The studied cases were in the domain of UTLs, which means that the layers were not thick enough to reach stability on the energy depth profile. This comparison has limitations since the values published by [17] are macroscopic measurements. Since there were no SP data available on literature in the simulated conditions presented on this chapter, the strategy was to compare the data considering ESTAR [17] value as a limit to the tendency curve evaluated as electron range (**Table 2**). Values above this limit were considered inconsistent for the simulation.

As can be seen on **Table 2**, only the electron range presented by DNAopt1 is above the macroscopic limit turning this the unique physics list that can be considered unreliable. Another important observation is that DNAopt2 and DNAopt3, and DNAopt4 and DNAopt5 presented similar electrons ranges due to the similarity on their transport models for electrons in energy range of this simulation (**Figure 2**).

The DNAopt1 simulates more electrons interactions (increasing the running time) than DNAopt4 and DNAopt5 that were the fastest among all physics lists

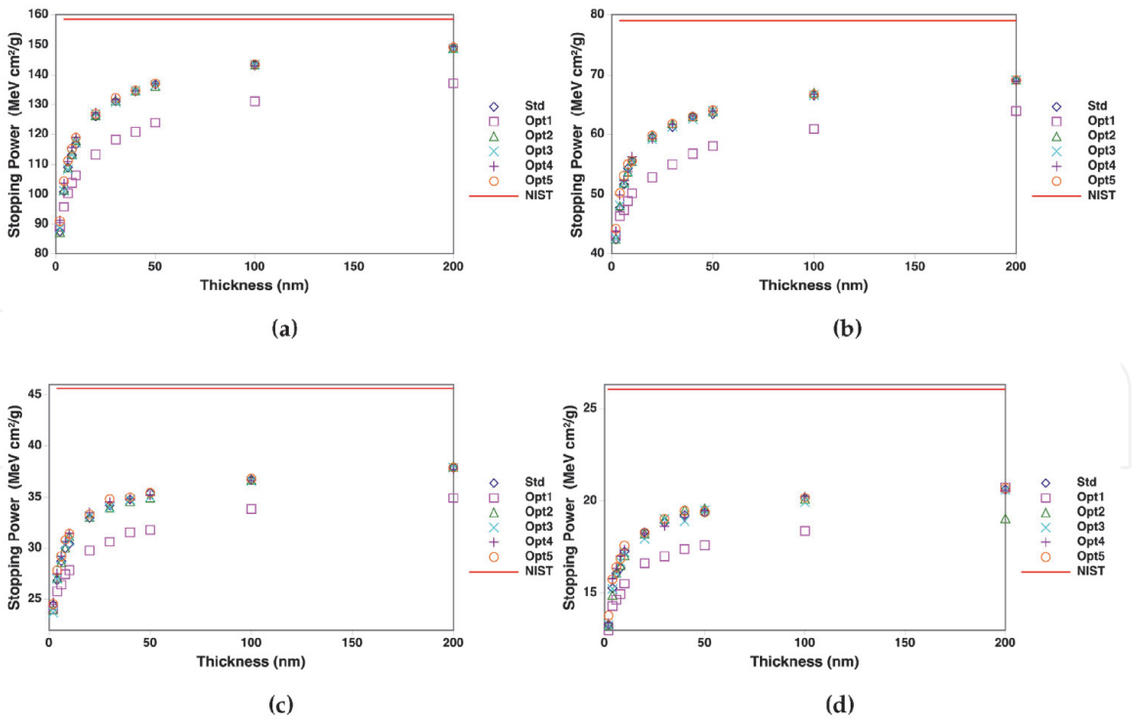

Figure 6.
Stopping power behaviour as function of the UTL thickness for different incident energy: 2 MeV (a), 5 MeV (b), 10 MeV (c) and 20 MeV (d). The red line represents the expected value of stopping power from PSTAR-NIST [19].

K_{proton}	2 MeV	5 MeV	10 MeV	20 MeV
K_{max}	4.34 keV	10.92 keV	21.90 keV	44.03 keV
std	380.41	1336.06	2917.06	10226.08
opt1	1409.78	4556.32	14524.03	7495.98
opt2	393.53	1246.24	3573.87	28166.71
opt3	385.60	1300.47	3911.23	13049.32
opt4	416.72	1513.44	4586.29	19025.65
opt5	415.67	1625.90	4281.31	15316.91
NIST	**581.61**	**2937.84**	**10060.36**	**34562.29**

1. K_{proton} represents the incident protons kinetic energy that will interact with the atomic electrons.
2. K_{max} represents the maximum kinetic energy that can be transferred in a head-on collision with an atomic electron.

Table 2.
Electrons range estimated with the simulated data and defined using NIST ESTAR [17].

evaluated. It was observed, for the simulated energies, that DNAopt1 was 1.5 to 4.1 more time consuming than DNA.

The tendencies, similarities and differences showed by the results obtained with the different physics lists can be explained reporting to the scheme on **Figure 2**. In this Figure one can see that: * DNAopt1 evokes the multiple scattering class for electrons instead of the elastic scattering (DNA) class for electrons; * DNAopt2 and DNAopt3 evoke the same process and model classes with the only change on the ionization model that had the flag SelectFasterComputer activated on DNAopt2; * DNAopt4 and DNAopt5 evoke similar process and model classes with exception for energy above 10 keV where additional models were evoked for excitation and ionization processes and the flag SelectFasterComputer was activated on DNAopt5.

2.4 The physics lists comparison

On this subsection the methodological strategy used and the comparisons among results of deposited energy profiles, total deposited energy and number of interactions for different Geant4-DNA physics lists is presented and analysed.

All statistical comparisons among different physics lists were performed using two-sample non-parametric statistical tests: Chi-Square test (χ^2) considering the statistical fluctuation of the simulation, independence Anderson-Darling k-Sample test (AD) and Kolmogorov–Smirnov (KS) test to evaluate both profiles distributions. The evaluation of the general conformity of the DNApto physics lists to the reference DNA physics list was performed by Chi-Square contingency Tables (CT) based on the number of cases that passed and failed the statistical χ^2 test. The contingency tables were applied to the total deposited energy and the depth and radial profile evaluations. All the statistical tests were performed for a significance level (SL) of 0.05.

2.4.1 The comparison findings

Figure 7 presents an example of radial and depth profiles according to DNA physics list that exemplifies the behaviour observed in all cases.

The shape of both profiles presented on **Figure 7** is similar to the expected. Usually, depth profiles show a Bragg Peak when the depth is thick enough to stop the incident particle [20]. This consideration cannot be applied in this study case since even the largest thickness evaluated is smaller than the protons and electrons range. Also, for UTLs the influence of the surface properties becomes significant due to the particles that are able to escape from it. In what follows, one may expect a small reduction on deposited energy at entrance surface and then an increase on the deposited energy as function of the depth until it reaches the stability around the range of the particles of interest (in this study case specially electrons). This behaviour is compatible with the example shown on **Figure 7a**. For radial profile one may expect the proportionality $E_{abs} \propto \frac{1}{r^n}$, where r represents the radius which means the distance from the center of the transported protons core and the position of the energy absorption, and $n \approx 2$. However, the n values presented by the simulations are slightly larger than 2 when the data presented on **Figure 6** are fitted to the proportionality equation. The same behaviour was reported by [21] on his validation of radial profiles with Geant4-DNA where this general tendency for the profiles was observed in all cases analysed and n was in the range of 2.1 to 2.38.

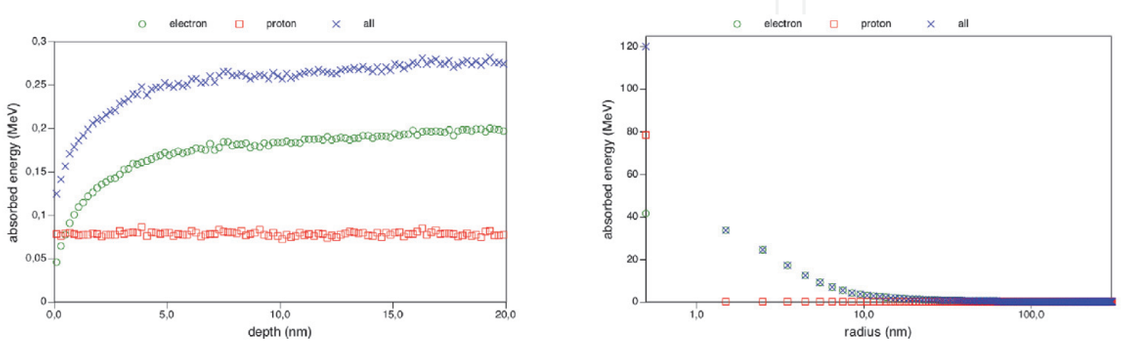

Figure 7.
Example of depth (a) and radial profile (b) simulated considering protons of 2 MeV passing through 20 nm water UTL by evoking DNA (stable) physics list.

The curves on **Figure 8** show a visual comparison among different transport models evoked. These curves exemplify the behaviour observed for all incident energies and UTL thicknesses. All models presented behaviour similar to the DNA physics list, with the exception of DNAopt1 where the depth profile showed a peak at the end of the water UTL.

Both depth and radial profiles showed lower energy deposition for DNAopt1 when compared to the other physics lists, indicating larger range for the secondary electrons generated by DNAopt1. Also, both profiles presented a localised deposited energy, evident on depth profile (at the end of the exit surface of the water ultra-thin layer) and diluted on the radial profile (near the core). The difference on the particles range (secondary electrons) can be noticed on **Figure 9**, where the DNA presented a smaller electron range when compared to the one showed by DNAopt1. DNAopt2,3,4 and 5 showed a similar behaviour to DNA physics list. Further investigation and statistical analysis are needed to generalize these results and evaluate the significance of these observations.

Tables 3 and **4** present the statistical tests p-values for depth profile by protons and electrons generated with different possible optional physics lists when compared to DNA physics list.

On **Table 3**, for protons, when the DNAopts are compared to DNA physics list, it is observable that χ^2 p-values are always higher than the SL with exception of DNAopt1 considering 2 MeV for thickness 6 nm and 5 MeV for 4 nm, as well as, one case on the limit of SL for 10 MeV and 200 nm. AD and KS statistical tests presented distributions significantly different when 100 nm and 200 nm were evaluated. Since χ^2 test evaluates the fluctuations on average value and the AD and KS tests evaluate the distribution considering only the average data, it reveals that the average data has some differences but they are not significant when the statistical

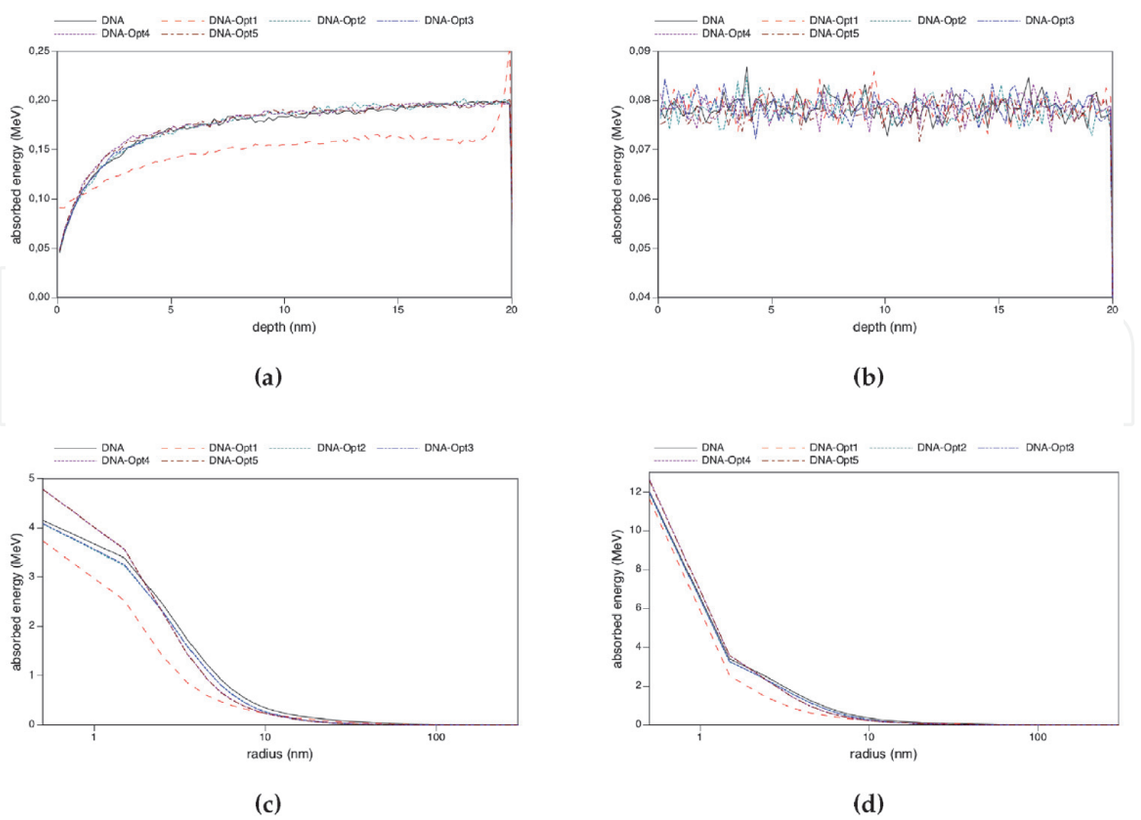

Figure 8.
Example of comparisons among different physics lists evoked on depth (a,b) and radial (c,d) profiles considering the deposited energy by secondary electrons (a,c) and protons (b,d) for incident protons of 2 MeV passing through 20 nm water UTL.

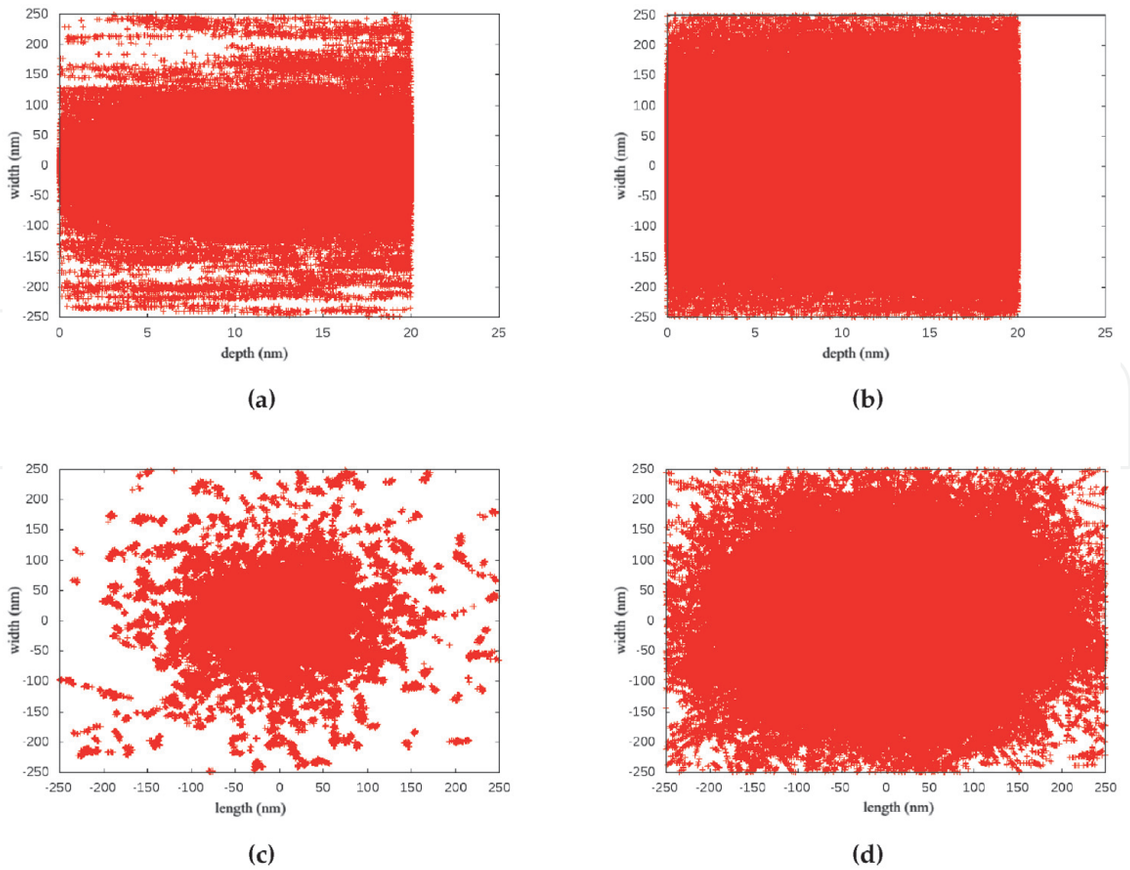

Figure 9.
Typical interaction maps as function of the depth (a,b) and radius (c,d) considering all particles for DNA (a, c), reference physics list and DNAopt1 (b,d) physics list for incident protons of 2 MeV passing through 20 nm water UTL.

Energy	Thickness	DNAopt1		DNAopt2		DNAopt3		DNAopt4		DNAopt5	
(MeV)	(nm)	AD	KS	AD	KS	AD	KS	AD	KS	AD	KS
2	10	0.0191	0.0243	0.0021	0.0008	—	—	—	—	—	—
	100	< 0.001	< 0.001	< 0.001	< 0.001	< 0.001	< 0.001	< 0.001	< 0.001	< 0.001	< 0.001
	200	< 0.001	< 0.001	< 0.001	< 0.001	< 0.001	< 0.001	< 0.001	< 0.001	< 0.001	< 0.001
5	8	—	—	< 0.001	< 0.001	< 0.001	< 0.001	—	—	—	—
10	8	—	—	—	—	< 0.001	< 0.001	—	—	—	—
20	8	< 0.001	< 0.001	—	—	—	—	—	—	—	—

Table 3.
Statistical evaluation of the energy depth profile for protons among the different physics list options when DNA physics lists is the reference, considering all studied cases, but showing only the cases with p-value inferior to 0.02.

fluctuations in each bin are taken into account. The contingency table evaluation shows 0.306 p-value when the physics list DNAopt1 is compared to DNA (higher than the SL). It happens because only few studied cases for DNAopt1 are significantly different from the reference DNA on the comparison among the evaluated physics lists. The physics lists DNAopt2,3,4 and 5 passed 100% of the statistical tests presenting no significant differences when compared to DNA physics list. The contingency table comparing all different optional physics lists presents p-value 0.3961, evidencing no significant difference from the reference physics list.

On **Table 4**, for electrons, when the DNAopts are compared to DNA physics list, it is observable that χ^2 p-values are always higher than the SL. However, for AD and

Energy	Thickness	DNAopt1		DNAopt2		DNAopt3		DNAopt4		DNAopt5	
(MeV)	(nm)	AD	KS	AD	KS	AD	KS	AD	KS	AD	KS
2	2	< 0.001	< 0.001	< 0.001	< 0.001	< 0.001	< 0.001	< 0.001	< 0.001	< 0.001	< 0.001
	6	< 0.001	< 0.001	—	—	—	—	—	—	—	—
	8	< 0.001	< 0.001	< 0.001	< 0.001	< 0.001	< 0.001	< 0.001	< 0.001	< 0.001	< 0.001
	10	< 0.001	< 0.001	—	—	—	—	—	—	—	—
	20	< 0.001	< 0.001	—	—	—	—	—	—	—	—
	40	< 0.001	< 0.001	—	—	—	—	—	—	—	—
	100	0.0019	0.0014	—	—	—	—	—	—	—	—
	200	< 0.001	< 0.001	—	—	—	—	—	—	—	—
5	2	< 0.001	< 0.001	0.0025	0.0010						
	6	< 0.001	< 0.001	—	—	—	—	—	—	—	—
	8	< 0.001	< 0.001	< 0.001	< 0.001	< 0.001	< 0.001	0.0050	0.0128		
	10	< 0.001	< 0.001	—	—	—	—	—	—	—	—
	20	< 0.001	< 0.001	—	—	—	—	—	—	—	—
	40	< 0.001	< 0.001	—	—	—	—	—	—	—	—
	50	< 0.001	< 0.001	—	—	—	—	—	—	—	—
	100	0.0023	< 0.001	—	—	—	—	—	—	—	—
	200	< 0.001	< 0.001	—	—	—	—	—	—	—	—
10	2	< 0.001	< 0.001	—	—	—	—	—	—	—	—
	6	< 0.001	< 0.001	—	—	—	—	—	—	—	—
	8	< 0.001	< 0.001	0.0739	0.0546	< 0.001	< 0.001	—	—	—	—
	10	< 0.001	< 0.001	0.0119	0.0132	0.0519	0.0727	0.0021	0.0016	0.0144	—
	20	< 0.001	< 0.001	—	—	—	—	—	—	0.0055	0.0028
	40	< 0.001	< 0.001	—	—	—	—	—	—	—	—
	50	< 0.001	< 0.001	—	0.0067	—	—	—	—	—	—
	100	0.0023	0.0014	—	—	—	—	—	—	—	—
	200	< 0.001	< 0.001	—	—	—	—	—	—	—	—
20	2	< 0.001	< 0.001	—	—	0.0042	0.0015	—	—	—	—
	6	< 0.001	< 0.001	—	—	< 0.001	< 0.001	—	—	—	—
	10	< 0.001	< 0.001	—	—	—	—	—	—	—	—
	20	< 0.001	< 0.001	—	—	—	—	0.0022	< 0.001	—	—
	30	—	0.0063	—	—	—	—	—	—	—	—
	40	< 0.001	< 0.001	0.0019	< 0.001	< 0.001	0.0016	—	—	0.0128	—
	50	< 0.001	< 0.001	—	—	—	—	—	—	—	—
	100	< 0.001	< 0.001	—	—	—	—	—	—	—	—
	200	< 0.001	< 0.001	—	—	—	—	—	—	—	—

Table 4.
Statistical evaluation of the energy depth profile for electrons among the different physics list options when DNA physics lists is the reference, considering all studied cases, but showing only the cases with p-value inferior to 0.02.

KS statistical tests the physics list DNAopt1 generally shows p-values lower than the SL, presenting significant differences in most cases when compared to DNA physics list. Again, it shows that the average data has some differences but they are not

significant when the statistical fluctuations of each bin are taken into account. Considering the χ^2, all the optional physics lists passed 100% of the statistical tests presenting no significant differences when compared to the reference physics list with the statistical fluctuations in the evaluation.

The statistical evaluation shows that despite the visible systematic differences represented on the **Figure 8**, those are not significant. Nevertheless, it is important to consider these systematic differences when one is studying depth profiles on a sensitive case, and it would be better to use any other physics list than DNAopt1, to avoid the influence of the changes in shape and the systematic lower energy deposition on the results.

It is not possible to statistically evaluate the proton radial profile because almost 100% of the energy is deposited on the first bin so, on **Table 5**, only the deposited energy radial profile for electrons is presented. It is observable that χ^2 p-values are always higher than the SL. The physics list DNAopt1 presents significant differences

Energy	Thickness	DNAopt1		DNAopt2		DNAopt3		DNAopt4		DNAopt5	
(MeV)	(nm)	AD	KS	AD	KS	AD	KS	AD	KS	AD	KS
2	4	< 0.001	< 0.001	—	—	—	—	—	—	—	—
	6	0.0032	0.0187	—	—	—	—	—	—	—	0.0033
	10	0.0034	0.0118	—	—	—	—	—	—	—	—
	20	0.0143	—	—	—	—	—	—	—	—	—
	30	< 0.001	< 0.001	—	—	—	—	—	—	—	—
	100	< 0.001	< 0.001	—	—	—	—	—	—	—	—
	200	< 0.001	< 0.001	—	—	—	—	—	—	—	—
5	2	< 0.001	< 0.001	0.0025	0.0010	—	—	—	—	—	—
	6	< 0.001	< 0.001	—		—	—	—	—	—	—
	8	< 0.001	< 0.001	< 0.001	< 0.001	< 0.001	< 0.001	0.0050	0.0128	—	—
	10	< 0.001	< 0.001	—	—	—	—	—	—	—	—
	20	< 0.001	< 0.001	—	—	—	—	—	—	—	—
	40	< 0.001	< 0.001	—	—	—	—	—	—	—	—
	50	< 0.001	< 0.001	—	—	—	—	—	—	—	—
	100	0.0020	< 0.001	—	—	—	—	—	—	—	—
	200	< 0.001	< 0.001	—	—	—	—	—	—	—	—
10	4	< 0.001	< 0.001	—	—	—	—	—	—	—	—
	30	< 0.001	< 0.001	—	—	—	—	—	—	—	—
	100	0.0012	0.0092	—	—	—	—	—	—	—	—
	200	< 0.001	0.0072	—	—	—	0.0092	—	—	—	—
20	4	< 0.001	< 0.001	—	—	—	—	0.0104	—	0.0094	0.0235
	6	< 0.001	0.0033	—	—	—	—	—	—	—	—
	20	< 0.001	0.01176	—	—	—	—	—	—	—	—
	30	< 0.001	< 0.001	—	—	—	—	—	—	—	—
	100	< 0.001	0.0019	—	—	—	—	—	—	—	—
	200	0.0016	0.0118	—	—	—	—	—	—	—	—

Table 5.
Statistical evaluation of the energy radial profile for electrons among the different physics list options when DNA physics lists is the reference, considering all studied cases, but showing only the cases with p-value inferior to 0.02.

in at least 50% of cases when compared to DNA physics list for all evaluated energies on AD and KS statistical tests. Once more, it shows that average data differences are not significant when the statistical fluctuations of each bin are taken into account. The optional physics lists passed 100% of the statistical tests presenting no significant differences when compared to DNA physics list.

The number of interactions of protons and electrons for all evaluated physics lists is presented on **Figure 10**. To analyse the data presented on **Figure 10** it is necessary to consider that on Monte Carlo simulation, as it is performed on Geant4-DNA, the increase on the number of interactions represents consequently an increase on running time.

It is easy to observe that, for the energy range studied, there is no significant change on the number of proton interactions. This can be explained by the processes and models evoked in the energy range of this study case, where incident protons transfer a few eV of their kinetic energy to electrons. Considering the energy range of incident protons, it can be seen on **Figure 1** that the process and model classes evoked by all physics lists evaluated were G4DNAExcitation process with G4DNABornExcitationModel, G4DNAIonisation process with G4DNABornIonisationModel and G4DNAChargeDecrease process with G4DNADingfelderChargeDecreaseMode. The only difference was the activation of the flag "SelectFasterComputation" for ionization transport of DNAopt2.

On the other hand, the number of electrons interactions presents significant changes.The observable differences for different physics lists can be justified by the different process and models evoked for electrons presented on **Figure 2**. DNAopt1 presents larger number of electrons interactions for thicknesses larger than 40 nm with the exception of 20 MeV incident kinetic energy protons beam where the DNAopt2 presents a number of electrons interactions similar to DNAopt1. This behaviour can be explained by the process and model classes evoked by all physics lists evaluated and the maximum kinetic transferred energy to the electrons which was estimated [14] as 4.34 keV for incident protons of 2 MeV, 10.92 keV for incident protons of 5 MeV, 21.90 keV for incident protons of 10 MeV and 44.03 keV for incident protons of 20 MeV. Under these conditions, all transport process classes can be evoked for electrons G4DNAElastic (for DNA and DNAopt2,3,4,and 5) or G4eMultipleScattering (for DNAopt1), G4DNAExcitation, G4DNAIonisation, G4DNAVibExcitation and G4DNAAttachment.

The main difference among the DNAopt1 and the other physics lists is the scattering process and model classes evoked that were a multiple scattering process and model instead of the discrete elastic process class implemented on Geant4-DNA. Taking DNA as reference, one may see that the scattering model was the only one that changed on the DNAopt1 implementation, so the high discrepancies observed on the number of electrons generated, deposited energy and electron

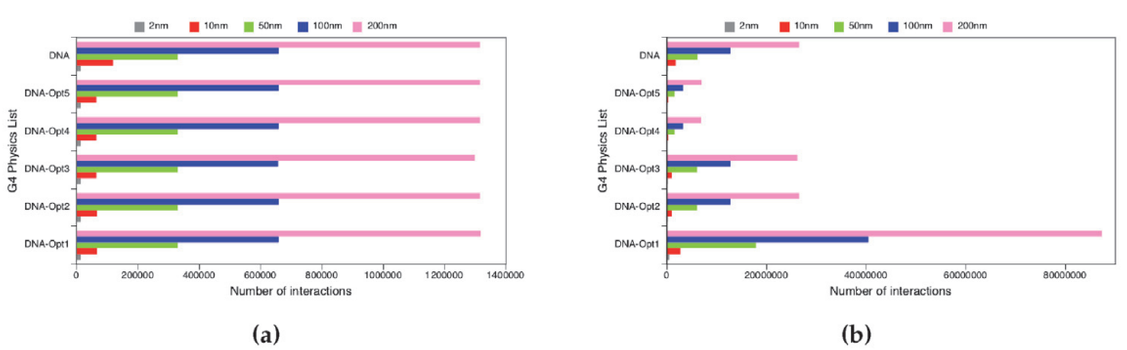

Figure 10.
Number of interactions for protons (a) and for electrons (b) considering incident protons of 10 MeV and different thicknesses of UTLs.

range are related to the implementation of the G4eMultipleScattering process class and the G4LowEWentzelVIModel model class. The physics lists DNAopt2 and DNAopt3 evoked the same process and model classes as DNA with the exception of DNAopt2 in ionization process where the flag "SelectFasterComputation" was activated. DNAopt4 and DNAopt5 evoked the same model as DNA for the process classes G4DNAVibExcitation and G4DNAAttachment; however, the other process classes G4DNAElastic, G4DNAExcitation and G4DNAIonisation models were different from DNA. Besides that, DNAopt5 process classes G4DNAExcitation and G4DNAIonisation evoked two models to each process, one additional model than the evoked by DNAopt4 for energies above 10 keV.

Taking the DNA physics list as reference, one can see that DNAopt1 presents a larger number of interactions for electrons. Considering the whole dataset simulated, all thicknesses and energies evaluated: DNAopt1 presents 1.5 to 4.1 times interactions; DNAopt2 and DNAopt3 present 0.5 to 1.0 times interactions; and DNAopt4 and DNAopt5 present 0.15 to 0.35 times interactions. The similar behaviour presented by DNAopt2 and DNAopt3 and by DNAopt4 and DNAopt5 was expected due to the similarities on the physics lists evoked to transport the secondary particles (electrons) in the energy range (**Figure 2**).

Figure 11 presents the graphics of the relative differences in the total deposited energies considering the DNA physics list as reference. It is easy to observe that DNAopt1 physics list presents the lowest average total deposited energy, 3rd and 4th quartiles and the largest standard deviation in all cases. This is in agreement to the observed energy depth and radial profiles where the DNAopt1 presents the lowest deposited energy (**Figure 7**).

Table 6 shows the statistical evaluation of the total deposited energy per ultrathin layers presenting χ^2, AD and KS p-values. These values are always higher than the SL for all optional physics list with the exception of DNAopt1 which presents all p-values below the SL. The contingency table for different incident kinetic kinetic energy protons beams presents p-value of 0.0016 (lower than the SL) for DNAopt1 when compared to each of the other optional physics lists. The evaluation of the

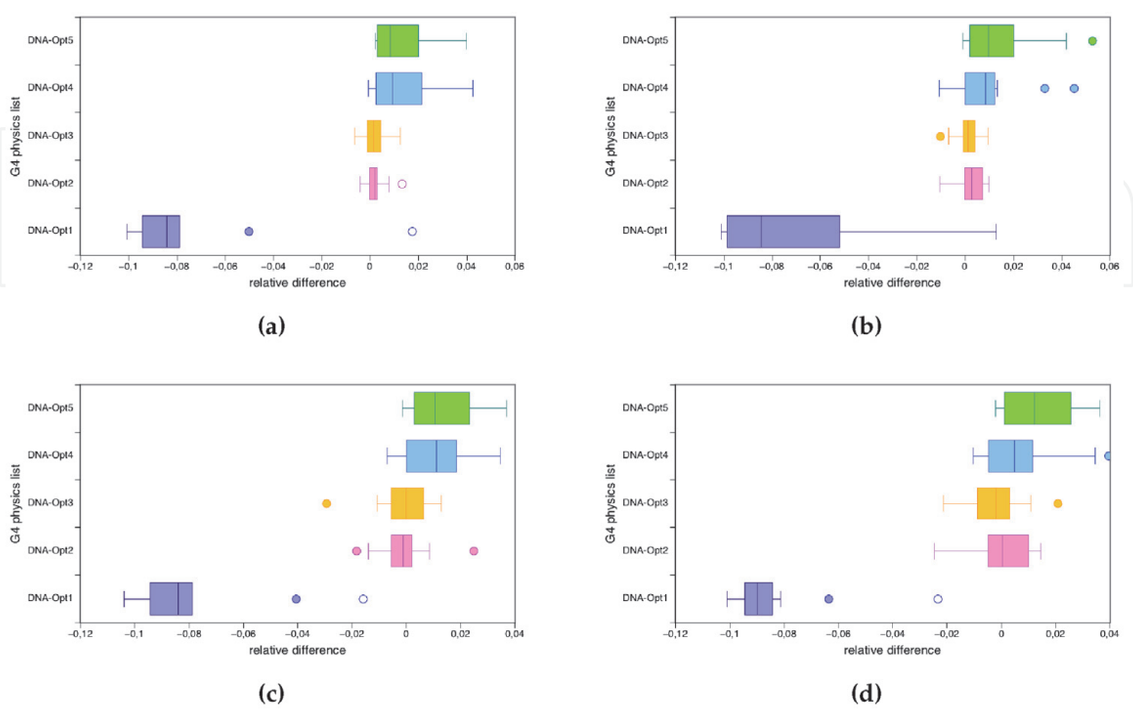

Figure 11.
Box-and-Whisker plots of the relative difference on total deposited energy on UTL considering all cases for incident kinetic energy protons beam of 2 MeV (a), 5 MeV (b), 10 MeV (c) and 20 MeV (d).

	DNAopt1			DNAopt2			DNAopt3		
Energy	χ^2	**AD**	**KS**	χ^2	**AD**	**KS**	χ^2	**AD**	**KS**
All Energies	0.0001	0.0444	0.0449	0.1195	1.0000	1.0000	0.0850	1.0000	1.0000
2 MeV	0.0001	0.0455	0.0449	1.0000	1.0000	1.0000	1.0000	1.0000	1.0000
5 MeV	0.0461	0.0490	0.0449	1.0000	1.0000	1.0000	1.0000	1.0000	1.0000
10 MeV	0.0430	0.0333	0.0449	0.9988	1.0000	1.0000	0.9402	1.0000	1.0000
20 MeV	0.0010	0.0395	0.0449	0.0573	1.0000	1.0000	0.5401	1.0000	1.0000

	DNAopt4			DNAopt5		
Energy	χ^2	**AD**	**KS**	χ^2	**AD**	**KS**
All Energies	1.0000	1.0000	1.0000	1.0000	1.0000	1.0000
2 MeV	1.0000	1.0000	1.0000	1.0000	1.0000	1.0000
5 MeV	1.0000	1.0000	1.0000	1.0000	1.0000	1.0000
10 MeV	1.0000	1.0000	1.0000	1.0000	1.0000	1.0000
20 MeV	0.7128	1.0000	1.0000	0.8225	1.0000	1.0000

Table 6.
Statistical evaluation of the total deposited energy considering all studied cases.

deposited energy considering all optional physics lists and studied conditions presents p-value lower than 0.001 evidencing the significant difference among all models. Taking into account that only DNAopt1 presents p-values below the statistical significance when compared to the DNA physics list one may conclude that the DNAopt1 is the only physics list with significant difference among the optional physics lists.

To get closer to the characteristic of the experimental material used (PMMA) the influence of the water density change on the profiles was analysed. **Figure 12** presents the depth and radial profiles comparing dense to standard water. As expected, the dense water presents higher deposited energies. The statistical evaluation shows that that the significant difference on depth profile is mainly due to secondary electrons interactions. It was not possible to obtain the statistical evaluation of protons radial profile because its deposited energy is almost completely performed on first bin. The logarithmic scale applied on x axis of radial profile makes more evident the differences between the curves, since on linear scale these differences are not visible. The total deposited energy on dense water is always larger than the total deposited energy on standard water, usually 15–20% higher (as was expected).

Table 7 shows p-values for statistical evaluation depth profile for protons and electrons interactions comparing dense to standard water. For protons, the χ^2 p-values are above the SL and AD and KS tests show p-values smaller than the SL, which means that the systematic differences observed in **Figure 12b** are not significant. The differences observed for electrons, in **Figure 12a**, are significant in all studied cases when comparing dense to standard water. For electrons, it is observable that χ^2 p-values are always higher than the SL and AD and KS tests show difference for few cases when comparing dense to standard water. It shows that, again, the average data has some differences but they are not significant when the statistical fluctuations in each bin are taken into account. The contingency table presents significant agreement on depth profile for protons with p-value 0.982 and significant difference on depth profile for electrons with p-value lower than 0.001.

Table 7 shows the statistical evaluation of radial profile for electrons considering standard and dense water indicating no significant statistical differences with exception of AD and KS tests for 2 MeV with 20 nm and 100 nm thicknesses.

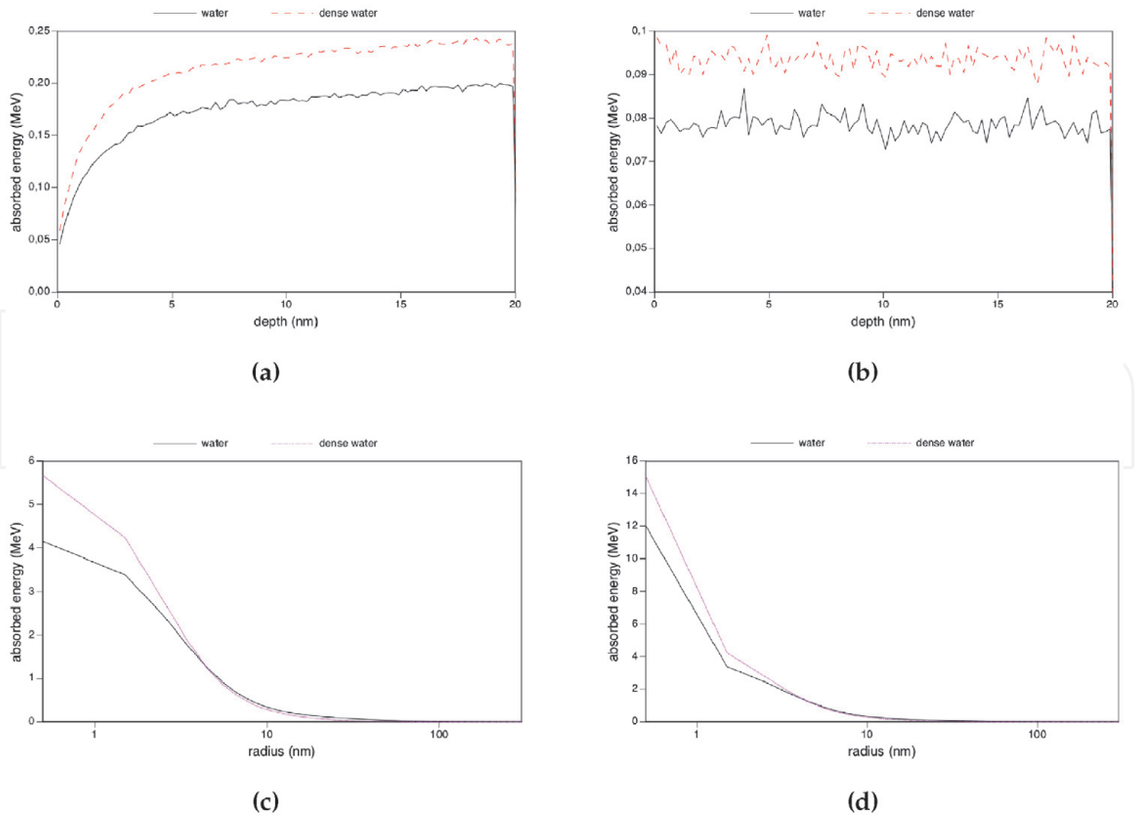

Figure 12.
Comparative depth (a,b) and radial (c,d) profiles of energy deposition due different particles: electrons (a,c), proton (b) and all particles (d).

Thickness	Depth profile for protons			Depth profile for electrons			Radial profile for electrons		
(nm)	χ^2	AD	KS	χ^2	AD	KS	χ^2	AD	KS
2	1.0000	< 0.001	< 0.001	0.0032	0.0881	0.2058	1.0000	0.2224	0.3505
4	1.0000	< 0.001	< 0.001	0.0219	0.0042	0.0063	1.0000	0.0937	0.0666
6	1.0000	< 0.001	< 0.001	0.0032	< 0.001	< 0.001	1.0000	0.2281	0.1163
10	1.0000	< 0.001	< 0.001	0.0010	< 0.001	< 0.001	1.0000	0.8888	0.6350
20	1.0000	< 0.001	< 0.001	0.0024	< 0.001	< 0.001	1.0000	0.0483	0.0362
30	1.0000	< 0.001	< 0.001	0.0210	< 0.001	< 0.001	1.0000	0.4578	0.3505
40	1.0000	< 0.001	< 0.001	0.0330	< 0.001	< 0.001	1.0000	0.2346	0.1163
50	1.0000	< 0.001	< 0.001	0.0043	< 0.001	< 0.001	1.0000	0.9351	0.5727
100	1.0000	< 0.001	< 0.001	0.0012	< 0.001	< 0.001	1.0000	< 0.001	< 0.001
200	1.0000	< 0.001	< 0.001	0.0032	< 0.001	< 0.001	1.0000	0.8697	0.9730

Table 7.
Statistical evaluation comparing the electrons and proton deposited energy depth profile and the electrons deposited energy radial profile for the standard water density to the water with PMMA density, considering all studied cases.

3. Final remarks

The evaluation of the CDCS (based on radial profile) showed that the bin size influences on the CDCS curve shapes. These results presented good agreement between the experimental CDCSs for polymer films and the simulated-calculated

values for standard water with 1 nm bin, despite different materials used. When the water density was augmented to the PMMA density value (dense water) the results became even more reliable.

In general, the SP values increased with the increase on the UTLs thickness, as expected, since the water layer thicknesses considered were smaller than the electron range. The simulated SP always presented lower values than NIST, as expected, with DNAopt1 generating the lowest (worst) SP values. Due to this behaviour the DNAopt1 presented unreliable electrons range values. This behaviour is probably due to the evocation of the multiple scattering process (with low energy Wenzel VI model) instead of the DNA elastic process.

Considering the reliability information presented in this chapter, all transport models available in Geant4-DNA presented reliable results for SP and CDCS with exception of DNAopt1. Further investigation is needed to map the differences among the possible physics lists available on Geant4-DNA.

In summary the comparison of energy deposition radial and depth profiles, taking DNA physics list as reference, showed that: (i) DNAopt2 to DNAopt5 presented similar results with percentage differences on simulated values lower than 8%; (ii) DNAopt1 presented the lowest deposited energy in both profiles when compared to the other physics lists, one peak at the end of the depth profile deposited energy, and a significant change on the curve shape on radial profile. In a general analysis the radial deposited energy decreased systematically in ultra-thin layers.

In a general evaluation, no significant differences were observed for the total deposited energy among all models, with exception of DNAopt1 which presented systematic distortions in the profile curves shape with a non-expected behaviour as confirmed by the contingency tables.

DNAopt1 showed itself being more time consuming and generated the lowest total deposited energy in UTLs, which resulted in the worst general agreement to the reference physics list DNA and to the expected data. It is important to emphasize that these conclusions are valid for the evaluated physics lists, energy range and geometrical conditions in this study and just for the Geant4-DNA (version 10.02. p01). Any other generalization requires further evaluation.

Acknowledgements

Research developed with the partial support of the National Supercomputing Center (CESUP), Federal University of Rio Grande do Sul (UFRGS).

Author details

Gabriela Hoff[1*], Raquel S. Thomaz[2], Leandro I. Gutierres[2], Sven Muller[2], Viviana Fanti[3], Elaine E. Streck[4] and Ricardo M. Papaleo[2]

1 National Institute for Nuclear Physics-Sezioni di Genova, Genova, GE, Italy

2 Interdisciplinary Center of Nanoscience and Micro-Nanotechnology, School of Technology, Pontifical Catholic University of Rio Grande do Sul, Porto Alegre, Brazil

3 Università di Cagliari and National Institute for Nuclear Physics-Sezioni di Cagliari, Monserrato, CA, Italy

4 Pontifical Catholic University of Rio Grande do Sul, Porto Alegre, Brazil

*Address all correspondence to: ghoff.gesic@gmail.com

References

[1] S. Agostinelli, J. Allison, K. a. Amako, J. Apostolakis, H. Araujo, P. Arce, M. Asai, D. Axen, S. Banerjee, G. . Barrand *et al.*, "Geant4a simulation toolkit," *Nuclear instruments and methods in physics research section A: Accelerators, Spectrometers, Detectors and Associated Equipment*, vol. 506, no. 3, pp. 250–303, 2003.

[2] J. Allison, K. Amako, J. Apostolakis, H. Araujo, P. A. Dubois, M. Asai, G. Barrand, R. Capra, S. Chauvie, R. Chytracek *et al.*, "Geant4 developments and applications," *IEEE Transactions on nuclear science*, vol. 53, no. 1, pp. 270–278, 2006.

[3] J. Allison, K. Amako, J. Apostolakis, P. Arce, M. Asai, T. Aso, E. Bagli, A. Bagulya, S. Banerjee, G. Barrand *et al.*, "Recent developments in geant4," *Nuclear Instruments and Methods in Physics Research Section A: Accelerators, Spectrometers, Detectors and Associated Equipment*, vol. 835, pp. 186–225, 2016.

[4] S. Incerti, A. Ivanchenko, M. Karamitros, A. Mantero, P. Moretto, H. Tran, B. Mascialino, C. Champion, V. Ivanchenko, M. Bernal *et al.*, "Comparison of geant4 very low energy cross section models with experimental data in water," *Medical physics*, vol. 37, no. 9, pp. 4692–4708, 2010.

[5] M. Bernal, M. Bordage, J. Brown, M. Davídková, E. Delage, Z. El Bitar, S. Enger, Z. Francis, S. Guatelli, V. Ivanchenko *et al.*, "Track structure modeling in liquid water: A review of the geant4-dna very low energy extension of the geant4 monte carlo simulation toolkit," *Physica Medica: European Journal of Medical Physics*, vol. 31, no. 8, pp. 861–874, 2015.

[6] S. Incerti, M. Douglass, S. Penfold, S. Guatelli, and E. Bezak, "Review of geant4-dna applications for micro and nanoscale simulations," *Physica Medica: European Journal of Medical Physics*, vol. 32, no. 10, pp. 1187–1200, 2016.

[7] *Guide For Physics Lists: release 10.4*, Geant4 Collaboration, 2017. [Online]. Available: http://geant4-userdoc.web.cern.ch/geant4-userdoc/UsersGuides/PhysicsListGuide/html/index.html

[8] G.-D. collaboration. The geant4-dna project: Extending the geant4 monte carlo simulation toolkit for radiobiology. [Online]. Available: geant4-dna.in2p3.fr/styled-3/styled-8/index.html

[9] G. Compagnini, R. Reitano, L. Calcagno, G. Marletta, and G. Foti, "Hydrogenated amorphous carbon synthesis by ion beam irradiation," *Applied Surface Science*, vol. 43, no. 1, pp. 228 – 231, 1989, beam Processing and Laser Chemistry. [Online]. Available: http://www.sciencedirect.com/science/article/pii/016943328990216X

[10] R. Barillon, M. Fromm, R. Katz, and A. Chambaudet, "Chemical Bonds Broken in Latent Tracks of Light Ions in Plastic Track Detectors," *Radiation Protection Dosimetry*, vol. 99, no. 1-4, pp. 359–362, 06 2002. [Online]. Available: https://doi.org/10.1093/oxfordjournals.rpd.a006802

[11] A. Licciardello, M. Fragal, G. Compagnini, and O. Puglisi, "Cross section of ion polymer interaction used to individuate single track regime," *Nuclear Instruments and Methods in Physics Research Section B: Beam Interactions with Materials and Atoms*, vol. 122, no. 3, pp. 589 – 593, 1997, nanometric Phenomena Induced by Laser, Ion and Cluster Beams. [Online]. Available: http://www.sciencedirect.com/science/article/pii/S0168583X96007550

[12] R. M. Papaléo, A. Hallén, B. U. R. Sundqvist, L. Farenzena, R. P. Livi, M.

A. de Araujo, and R. E. Johnson, "Chemical damage in poly(phenylene sulphide) from fast ions: Dependence on the primary-ion stopping power," *Phys. Rev. B*, vol. 53, pp. 2303–2313, Feb 1996. [Online]. Available: https://link.aps.org/doi/10.1103/PhysRevB.53.2303

[13] R. Papalo, L. Farenzena, M. de Arajo, R. Livi, M. Alurralde, and G. Bermudez, "Cratering in pmma induced by gold ions: dependence on the projectile velocity," *Nuclear Instruments and Methods in Physics Research Section B: Beam Interactions with Materials and Atoms*, vol. 148, no. 1, pp. 126 – 131, 1999. [Online]. Available: http://www.sciencedirect.com/science/ article/pii/S0168583X98008775

[14] R. Thomaz, P. Louette, G. Hoff, S. Müller, J. J. Pireaux, C. Trautmann, and R. M. Papaléo, "Bond-breaking efficiency of high-energy ions in ultrathin polymer films," *Phys. Rev. Lett.*, vol. 121, p. 066101, Aug 2018. [Online]. Available: https://link.aps.org/doi/10.1103/ PhysRevLett.121.066101

[15] G.-D. Collaboration. (2018) Geant4 cross reference. [Online]. Available: http://www-geant4.kek.jp/lxr/source/

[16] U. Hossain, V. Lima, O. Baake, D. Severin, M. Bender, and W. Ensinger, "On-line and post irradiation analysis of swift heavy ion induced modification of pmma (polymethyl-methacrylate," *Nuclear Instruments and Methods in Physics Research Section B: Beam Interactions with Materials and Atoms*", vol. 326, pp. 135 – 139, 2014, 17th International Conference on Radiation Effects in Insulators (REI). [Online]. Available: http://www.sciencedirect.com/ science/article/pii/S0168583X14000950

[17] N.-N. I. of Standards and Technology. (2009) Estar: stopping power and range tables for electrons. [Online]. Available: https://physics.nist.gov/ PhysRefData/Star/Text/ESTAR.html

[18] F. H. Attix, *Introduction to radiological physics and radiation dosimetry*. John Wiley & Sons, 1986.

[19] N.-N. I. of Standards and Technology. (1998) Pstar: stopping power and range tables for protons. [Online]. Available: https://physics.nist.gov/PhysRefData/Star/Text/PSTAR.html

[20] R. Garcia-Molina, I. Abril, P. de Vera, I. Kyriakou, and D. Emfietzoglou, "A study of the energy deposition profile of proton beams in materials of hadron therapeutic interest," *Applied Radiation and Isotopes*, vol. 83, pp. 109–114, 2014.

[21] H. Wang and O. N. Vassiliev, "Radial dose distributions from protons of therapeutic energies calculated with geant4-dna," *Physics in Medicine & Biology*, vol. 59, no. 14, p. 3657, 2014.